Distinct conformations of in vitro and in vivo amyloids of huntingtin-exon1 show different cytotoxicity

Yoko Nekooki-Machida[a], Masaru Kurosawa[b], Nobuyuki Nukina[b], Kazuki Ito[c], Toshiro Oda[c], and Motomasa Tanaka[a,d,1]

[a]Tanaka Research Unit, [b]Laboratory for Structural Neuropathology, RIKEN Brain Science Institute, Hirosawa 2-1, Wako, Saitama 351-0198, Japan; [c]RIKEN SPring-8 Center, 1-1-1 Kouto, Sayo, Hyogo 679-5148, Japan; and [d]PRESTO, Japan Science and Technology Agency, Honcho 4-1-8, Kawaguchi, Saitama 332-0112, Japan

Edited by David S. Eisenberg, University of California, Los Angeles, CA, and approved April 17, 2009 (received for review November 26, 2008)

A hallmark of polyglutamine diseases, including Huntington disease (HD), is the formation of β-sheet-rich aggregates, called amyloid, of causative proteins with expanded polyglutamines. However, it has remained unclear whether the polyglutamine amyloid is a direct cause or simply a secondary manifestation of the pathology. Here we show that huntingtin-exon1 (thtt) with expanded polyglutamines remarkably misfolds into distinct amyloid conformations under different temperatures, such as 4 °C and 37 °C. The 4 °C amyloid has loop/turn structures together with mostly β-sheets, including exposed polyglutamines, whereas the 37 °C amyloid has more extended and buried β-sheets. By developing a method to efficiently introduce amyloid into mammalian cells, we found that the formation of the 4 °C amyloid led to substantial toxicity, whereas the toxic effects of the 37 °C amyloid were very small. Importantly, thtt amyloids in different brain regions of HD mice also had distinct conformations. The thermolabile thtt amyloid with loop/turn structures in the striatum showed higher toxicity, whereas the rigid thtt amyloid with more extended β-sheets in the hippocampus and cerebellum had only mild toxic effects. These studies show that the thtt protein with expanded polyglutamines can misfold into distinct amyloid conformations and, depending on the conformations, the amyloids can be either toxic or nontoxic. Thus, the amyloid conformation of thtt may be a critical determinant of cytotoxicity in HD.

Huntington disease | polyglutamine misfolding | aggregation

Huntington disease (HD) is an autosomal, dominantly inherited neurodegenerative disorder with a typical onset in mid-life (1). HD is characterized by motor dysfunction, memory deficit, and personality changes, including depression. One of the striking features in HD is severe atrophy of the caudate and putamen (2, 3). Cerebral cortical atrophy is also common, whereas cerebellar Purkinje cell loss occurs only in juvenile-onset cases. The pathological gene product of HD is a functionally enigmatic huntingtin (htt) protein, and the CAG repeat in htt-exon1 is expanded to >36 in HD (1). A translated, expanded polyglutamine in mutant htt renders the protein prone to aggregation because of the insoluble nature of the expanded polyglutamines. The polyglutamine aggregates show β-sheet-rich fibrillar structures, termed amyloid, in vitro (4, 5). The amyloid structure of polyglutamine aggregates is also observed in a mouse model of HD and in brains of HD patients (6, 7).

Although the aggregate formation of responsible proteins with expanded polyglutamines is a characteristic of polyglutamine diseases, including HD, it is unclear whether the polyglutamine aggregates themselves are toxic, that is, whether they are the cause or merely the result of the pathology (8, 9). Several studies have indicated that polyglutamine aggregates are connected with neurodegeneration or cytotoxicity (6, 7, 10, 11), whereas other studies have suggested that aggregate formation is either not intimately correlated with cytotoxicity (12–15) or plays a protective role in cells (16). This apparent inconsistency may be caused by structural diversity of amyloid, as amyloid-forming proteins often misfold into more than 1 conformation and the phenotypic and pathologic consequence of harboring aggregates depends critically on the specific amyloid form a protein adopts (17–21). A striking example of this observation is the prion strain phenomenon. Accumulating evidence from both yeast and mammalian prions argues that differences in the prion conformation underlie distinct phenotypic states in prion strain variants (19, 22). The amyloid-β 1–40 peptide, which is responsible for Alzheimer's disease, is also able to misfold into different amyloid conformations under specific conditions (23). The distinct amyloid forms showed differential toxicity when they were tested in primary rat embryonic hippocampal neurons. However, the toxic effects of specific amyloid conformations introduced *inside* mammalian cells remain unclear.

Here we demonstrate huntingtin-exon1 with expanded polyglutamines forms distinct amyloid conformations. By using a method to efficiently introduce amyloid into mammalian cells, we provide evidence for conformation-dependent cytotoxicity of in vitro and in vivo thtt amyloids. A flexible amyloid conformation with exposed β-sheets and loop/turn structures shows higher toxicity, whereas a rigid conformation containing extended and buried β-sheets has only small toxic effects. Identification of the toxic amyloid conformation may provide a therapeutic strategy for HD.

Results

Distinct Amyloid Conformations of in Vitro thtt Containing Expanded Polyglutamines. N-terminal polyhistidine- and GST-tagged thtt protein containing 10 (thttQ10), 42 (thttQ42), or 62 (thttQ62) glutamine repeats was expressed in *Escherichia coli* and purified. After cleavage of the tag, thttQ42 and thttQ62, but not thttQ10, spontaneously formed fibrillar aggregates termed amyloid, which bind to an amyloid-specific dye, thioflavine T (Fig. S1). Amyloid formation was also monitored by turbidity of the protein solution, and we observed a sigmoidal curve, which is similar to that seen in thioflavine T binding (Fig. S1).

Earlier studies have shown that amyloid-forming proteins can spontaneously adopt a variety of fiber types (19), suggesting that thtt with expanded polyglutamines may misfold into different amyloid conformations. We first sought to investigate the structural diversity of thtt amyloids in vitro simply by polymerizing thtt protein at either 4 °C or 37 °C. Electron microscopy (EM) indicated that both 4 °C and 37 °C amyloids were homogeneous, and their morphology looked similar (Fig. 1*A*). X-ray fiber diffraction showed that both

Author contributions: Y.N.-M. and M.T. designed research; Y.N.-M., K.I., T.O., and M.T. performed research; Y.N.-M., M.K., N.N., and M.T. contributed new reagents/analytic tools; Y.N.-M. and M.T. analyzed data; and Y.N.-M. and M.T. wrote the paper.

The authors declare no conflict of interest.

This article is a PNAS Direct Submission.

Freely available online through the PNAS open access option.

[1]To whom correspondence should be addressed. E-mail: motomasa@brain.riken.jp.

This article contains supporting information online at www.pnas.org/cgi/content/full/0812083106/DCSupplemental.

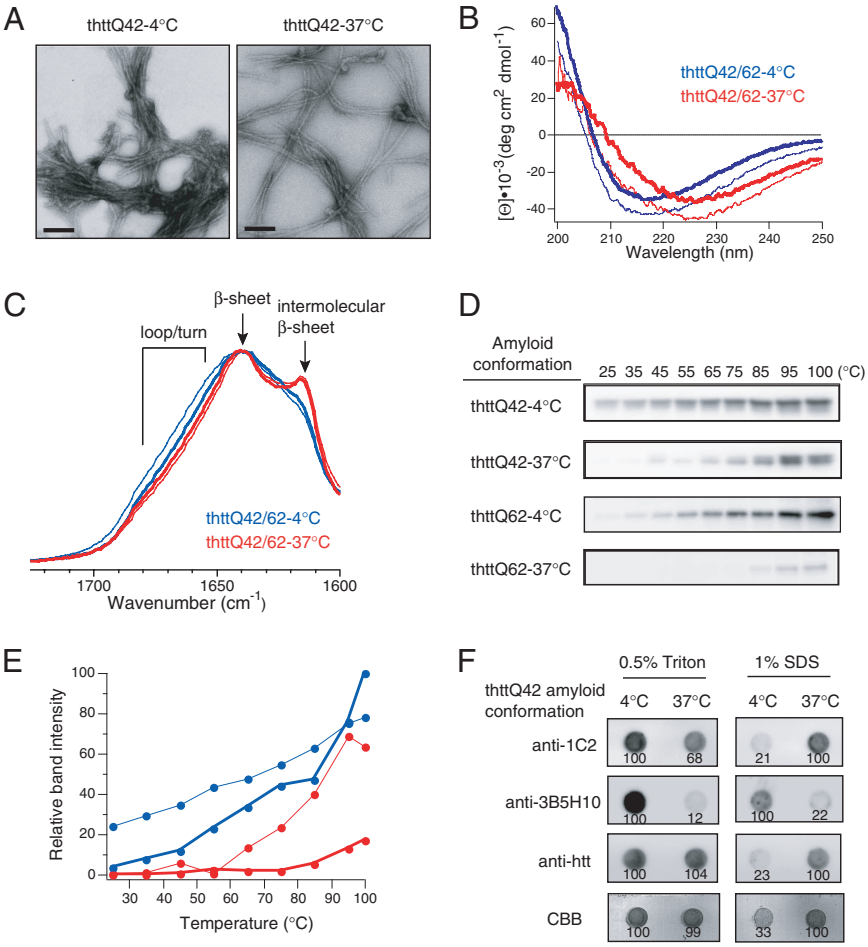

Fig. 1. thtt protein with expanded polyglutamines misfolds into distinct amyloid conformations in vitro. (*A*) EM images of thttQ42-4 °C and thttQ42-37 °C amyloids. (Scale bar, 100 nm.) (*B*) CD spectra of thttQ42-4 °C (thin, blue), thttQ42-37 °C (thin, red), thttQ62-4 °C (bold, blue), and thttQ62-37 °C (bold, red) amyloids. (*C*) FT-IR spectra of thttQ42-4 °C (thin, blue), thttQ42-37 °C (thin, red), thttQ62-4 °C (bold, blue), and thttQ62-37 °C (bold, red) amyloids. (*D*) Thermal stability of thttQ42-4 °C, thttQ42-37 °C, thttQ42-4 °C and thttQ42-37 °C amyloids. The bands indicate monomeric thttQ42/62 solubilized from thttQ42/62 amyloids by the heat treatment. (*E*) The band intensity in (*D*) was plotted against temperature for thttQ42-4 °C (thin, blue), thttQ42-37 °C (thin, red), thttQ62-4 °C (thick, blue), and thttQ62-37 °C (thick, red) amyloids. (*F*) Reactivity of thttQ42-4 °C and thttQ42-37 °C amyloids with various antibodies. A filter trap assay was performed in the presence of 0.5% Triton X-100 (*Left*) or 1% SDS (*Right*) and processed for immunoblotting against a 1C2, 3B5H10, or anti-htt antibody. Coomassie Brilliant Blue (CBB) staining is also shown below. Values show relative intensities of the spots.

conformations have β-sheet-rich structures (Fig. S2), which are typical of amyloid fibrils. However, we found that the 4 °C amyloid exhibited higher affinities for amyloid-binding dyes, thioflavine T and Congo red, than the 37 °C amyloid, suggesting some structural differences in the 2 amyloid conformations (Fig. S3).

We found structural differences in the 2 amyloid conformations by CD spectroscopy. The 4 °C and 37 °C amyloids showed spectra of classical β-sheet and extended β-sheet structures (Fig. 1*B*), which have a negative peak at 218 and 225 cm^{-1}, respectively (24). To examine the structural differences in more detail, we measured FT-IR spectroscopy. FT-IR spectra revealed that the 4 °C amyloid has some loop/turn structures (1,655–1,680 cm^{-1}), whereas the 37 °C amyloid contains more intermolecular β-sheets (1,615 cm^{-1}) (25, 26), in addition to the mostly β-sheet structures (1,640 cm^{-1}) in both amyloid conformations (Fig. 1*C*). We further explored physical properties of the distinct amyloids by investigating resistance of the amyloids to thermal denaturation and mechanical shearing. We first examined thermal stability of each amyloid conformation by quantifying amounts of monomeric thttQ42 solubilized from thttQ42 amyloid by heat treatment. The 2 amyloid forms of thttQ42 showed strikingly different thermal stabilities: The 4 °C amyloid was more thermolabile than the 37 °C amyloid (Fig. 1 *D* and *E* and Fig. S4). Next, we investigated the physical stability of the 2 amyloid conformations. Although both thttQ42 4 °C and 37 °C amyloids that were formed under an undisturbed condition showed similar long fibrils (Fig. 1*A*), 4 °C amyloids were more easily broken by agitation or sonication than 37 °C amyloids (Fig. S5). This result implied that the 4 °C amyloid was more fragile and thereby, more easily fragmented by mechanical forces. These results suggest that the 4 °C amyloid conformation is more fragile because of the presence of loop/turn structures, whereas the 37 °C conformation is more rigid due to the extended β-sheets.

Next we investigated conformations of polyglutamines in the 2 distinct amyloid forms by using the 1C2 antibody that preferentially recognizes exposed expanded polyglutamines but slightly reacts with buried polyglutamines (27, 28). In the filter trap assay using the antibody, we found that polyglutamines in the 4 °C amyloid were more reactive to the 1C2 antibody, whereas those in the 37 °C amyloid showed lower reactivity (Fig. 1*F*). In contrast, an antibody for huntingtin as well as Coomassie Brilliant Blue reacted similarly to both conformations. This result indicates that expanded polyglutamines in the 4 °C amyloid conformation are exposed and flexible enough to bind to the 1C2 antibody, whereas those in the 37 °C amyloid conformation are buried by forming more extended β-sheets and thereby less reactive to the antibody. Interestingly, the 4 °C amyloid conformation was more reactive to a 3B5H10 antibody that reacts with a toxic form of expanded polyglutamines (29) (Fig. 1*F*). We also verified in the dot blot that the 37 °C conformation is more resistant to SDS than the 4 °C conformation (Fig. 1*F*). In addition, we found the 4 °C and 37 °C amyloids show distinct fiber growth rates at 4 °C and 37 °C (Fig. S6). Taken together, these results establish that the thtt protein with expanded polyglutamines misfolds into different amyloid conformations with distinct physical properties.

Efficient Introduction of in Vitro thtt Amyloids into Mammalian Cells. To directly examine the cytotoxicity of the different amyloid conformations, we sought to develop a highly efficient and versatile protocol by which in vitro amyloids are introduced into mammalian cells without laborious microinjection (see *SI Text*). For mammalian

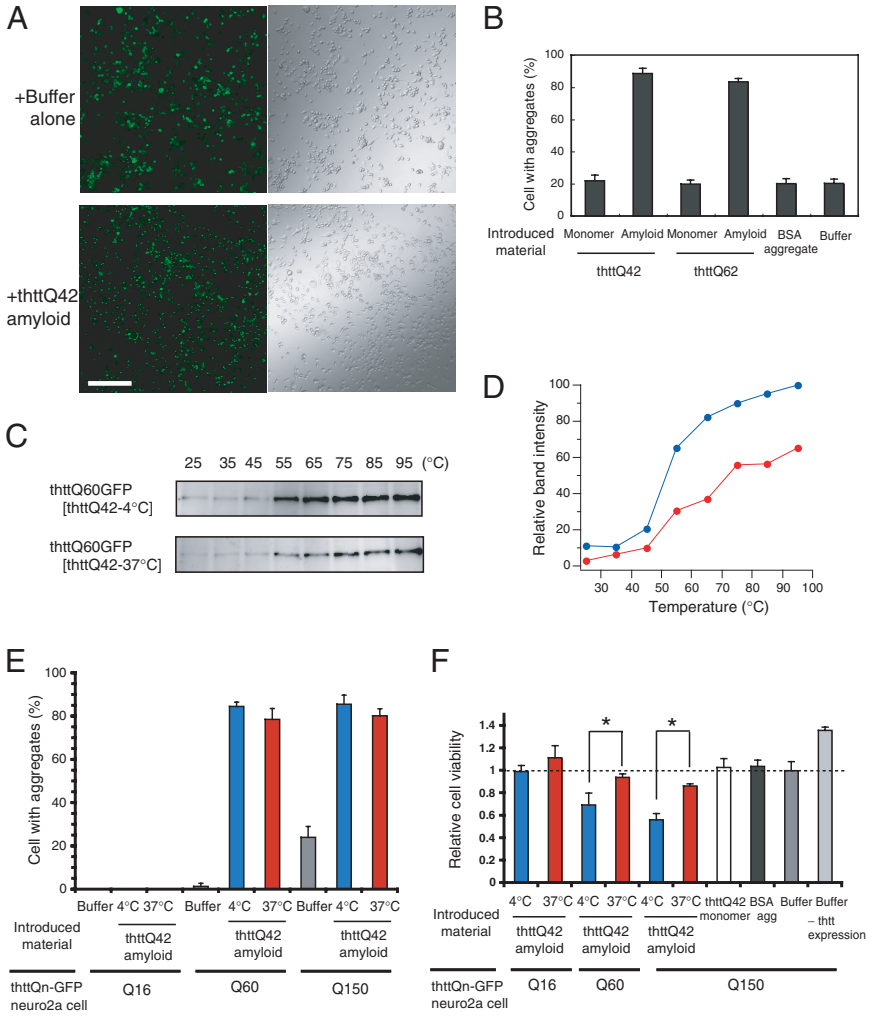

Fig. 2. Different conformations of thtt amyloids show distinct cytotoxicity in neuro2a cells. (*A*) Significant acceleration of thttQ150-GFP aggregation by introduction of in vitro thttQ42 amyloids. Buffer alone (*Upper*) or in vitro thttQ42 amyloids (*Lower*) were introduced into thttQ150-GFP stable neuro2a cells. Shown are fluorescent (*Left*) and DIC (*Right*) images of the thttQ150-GFP cells after 15 h of thttQ150-GFP expression and cell differentiation. (Scale bar, 250 μm.) (*B*) Buffer alone, GST-thttQ42 monomer, thttQ42 amyloids, GSTthttQ62 monomer, thttQ62 amyloids, or BSA aggregates were introduced into stable thttQ150-GFP neuro2a cells. The number of cells with thttQ150-GFP foci was counted after 15 h of the thttQ150-GFP expression and cell differentiation. Values are mean ± SD. (*C*) Thermal stability of the thttQ60-GFP amyloids formed in the presence of in vitro thttQ42-4 °C (thttQ60-GFP[thttQ42-4 °C]) or thttQ42-37 °C amyloid "seeds" (thttQ60-GFP[thttQ42-37 °C]). (*D*) The band intensity of thttQ60-GFP[thttQ42-4 °C] (blue) or thttQ60-GFP[thttQ42-37 °C] (red) amyloids in *C* was plotted against temperature. (*E*, *F*) Buffer alone, in vitro thttQ42-4 °C amyloids, thttQ42-37 °C amyloids, GSTthttQ42 monomer, or BSA aggregates were introduced into thttQ16-, Q60-, or Q150-GFP neuro2a cells under a regulatable promoter. The thtt expression and cell differentiation started after 3 h of the in vitro amyloid transduction. The number of cells with thtt-GFP foci was counted after 15 h (*E*) and cell viability was examined by MTT assay after 4 days of the thtt expression and cell differentiation (*F*). *, $P < 0.01$. Values are mean ± SD.

cells, we used stable neuro2a cells that overexpress thtt-GFP fusion protein containing Q16, Q60, or Q150 under a ponasterone-regulatable promoter (30). After extensive attempts, we succeeded in delivering thtt amyloids into the neuro2a cells efficiently by using a lipid-based procedure. First, in vitro thttQ42 amyloids were introduced into thttQ150-GFP cells, followed by induction of thttQ150-GFP expression and cell differentiation (30). We then estimated the aggregation status of the endogenous thtt-GFP after 15 h of thtt expression and cell differentiation. If in vitro thtt amyloids are successfully introduced into cells, they are expected to seed endogenous thtt-GFP protein and thereby enhance aggregation of thtt-GFP. Remarkably, we found that the introduction of thttQ42 amyloids significantly accelerated thtt150Q-GFP aggregation (Figs. 2*A* and S7*A*). GFP foci, because of the aggregation of thttQ150-GFP, were observed in more than 80% of GFP-positive cells, whereas only 15–20% of cells had GFP foci after the treatment of cells with buffer alone, which represents spontaneous aggregation of thttQ150-GFP on induction of the protein expression (Fig. 2*B*). Introduction of neither monomeric thtt nor BSA aggregates facilitated thttQ150-GFP aggregation, indicating that the seeding effects are specific to the thtt amyloid (Fig. 2*B*). A significant acceleration of thtt-GFP aggregation by introduction of in vitro thttQ42 amyloid was also observed in other neuronal PC12 cells in which both in vitro amyloids and plasmids encoding thtt-GFP were introduced at the same time (Fig. S8). Thus, our procedure for amyloid transduction is not limited to specific cells but is rather versatile. These results, together with colocalization of fluorescently labeled, in vitro thtt amyloids with thttQ150-GFP foci (Fig. S7*B*), establish that in vitro thtt amyloids are successfully introduced into mammalian cells and act as "seeds" inside cells.

Next we investigated whether the amyloid conformations of endogenous thtt-GFP maintain those of in vitro thtt amyloids that were introduced into cells. By extensive washing with SDS, we partially purified thttQ60-GFP amyloids, which were formed in the presence of in vitro thttQ42-4 °C or thttQ42-37 °C amyloid "seeds", in stable thttQ60-GFP neuro2a cells and analyzed their thermal resistance. We found that conformations of thttQ60-GFP amyloids in the neuro2a cells were similar to those of the in vitro thttQ42 amyloids that were introduced into cells (Fig. 2 *C* and *D*): thttQ60-GFP amyloids seeded by thttQ42-4 °C amyloids were more thermolabile, and those seeded by thttQ42-37 °C amyloids were thermally more stable, as observed for in vitro thttQ42-4 °C and thttQ42-37 °C amyloids, respectively. These results indicate that conformations of thtt amyloids faithfully propagate in mammalian cells, although slight differences in the thermal stability are observed between thttQ60-GFP amyloids and in vitro thttQ42 amyloids, which could be caused by the presence of aggregate-interacting proteins in the thttQ60-GFP amyloids or a GFP tag in thttQ60-GFP.

Cytotoxicity of Different Conformations of thtt Amyloids in Vitro. Our abilities to create distinct conformations of thtt amyloids and introduce them into mammalian cells allowed us to directly examine toxicity of specific amyloid conformations in mammalian cells. We

found that both 4 °C and 37 °C conformations of in vitro thtt amyloid significantly accelerated the aggregation of thtt-GFP compared with buffer alone (Fig. 2*E*). For both thttQ60-GFP and thttQ150-GFP neuro2a cells, each amyloid conformation of 4 °C and 37 °C enhanced the aggregation of endogenous thttQ60-GFP or thttQ150-GFP to similar levels (≈80%). In contrast, these amyloids did not induce aggregation of thttQ16-GFP (Fig. 2*E*).

We then examined cytotoxicity of these different thtt amyloids by a standard MTT assay (30). Although similar aggregation levels of thttQ60/Q150-GFP were observed by introduction of both 4 °C and 37 °C conformations, we found that these amyloid conformations led to different toxicities for both thttQ60-GFP and thttQ150-GFP neuro2a cells (Fig. 2*F*). The 4 °C amyloid conformation was more toxic, whereas the 37 °C conformation had milder effects. The toxic effects of the thtt amyloids were dose-dependent (Fig. S9), and both monomeric thtt and BSA aggregates did not show cytotoxicity (Fig. 2*F*), indicating that thtt amyloids are responsible for cytotoxicity. Importantly, both the 4 °C and 37 °C amyloid conformations showed neither induction of thtt aggregation nor toxicity in neuro2a cells overexpressing thttQ16-GFP (Fig. 2 *E* and *F*). These results indicate that thtt amyloids with expanded polyglutamines themselves are not intrinsically toxic, but rather a formation process of a specific thtt amyloid conformation such as thttQ42-4 °C leads to cell death. Taken together, the present results demonstrate that thtt with expanded polyglutamines can adopt distinct, self-propagating conformations, and that these conformational differences underlie distinct cytotoxicity.

Different Conformations of thtt Amyloids in HD Mice. Next, we investigated whether the conformational differences of in vitro thtt amyloids can be recapitulated in vivo. We purified thtt amyloids with SDS from a variety of brain regions, including cerebral cortex, striatum, hippocampus, and cerebellum, in the R6/2 transgenic mouse model of HD (31). The SDS-resistant thtt amyloids from R6/2 mice showed significant seeding effects on polymerization of in vitro thttQ42 protein, whereas corresponding insoluble fractions obtained from wild-type mice by the same procedure had only small effects (Fig. 3 *A* and *B*, see *SI Text* for more discussion). These results indicate that the thtt amyloids were successfully purified from R6/2 mice, and they worked as "seeds" for in vitro polymerization of thtt.

We then investigated conformational diversity of these thtt amyloids in vivo. The aggregates purified from R6/2 mice are not completely pure and thus, may not be suitable for structural analysis directly. However, conformations of in vivo thtt amyloids can be propagated by seeding reactions, as shown in Fig. 3 *C* and *D*. We amplified conformations of in vivo thtt amyloids by polymerizing in vitro thttQ42 in the presence of the amyloid "seeds" purified from R6/2 mice and used them for thermal stability and structural analyses. We found that thtt amyloids from the striatum were the most thermally labile, whereas those from the hippocampus and cerebellum showed higher resistance to heat treatment (Fig. 3 *C* and *D*). The thtt amyloids from the striatum showed the presence of loop/turn structures (1,655–1,680 cm^{-1}), whereas those from the hippocampus and cerebellum had more intermolecular β-sheets (1,615 cm^{-1}) in addition to the mostly β-sheet structures (1,640 cm^{-1}) (Fig. 3 *E* and *F*). Interestingly, these physical and structural properties of the thtt amyloids in the striatum and hippocampus/cerebellum resemble those of in vitro thtt 4 °C and 37 °C amyloids, respectively. These results indicate that thtt amyloids in different brain regions of HD mice have distinct conformations as observed for in vitro thtt amyloids.

Distinct Cytotoxicity of Different Conformations of thtt Amyloids in HD Mice. Next, we examined effects of these distinct in vivo amyloid conformations on thtt aggregation and cell viability by directly introducing these amyloids into neuro2a cells by using our amyloid transduction protocol. We found that thtt amyloids from R6/2 mice

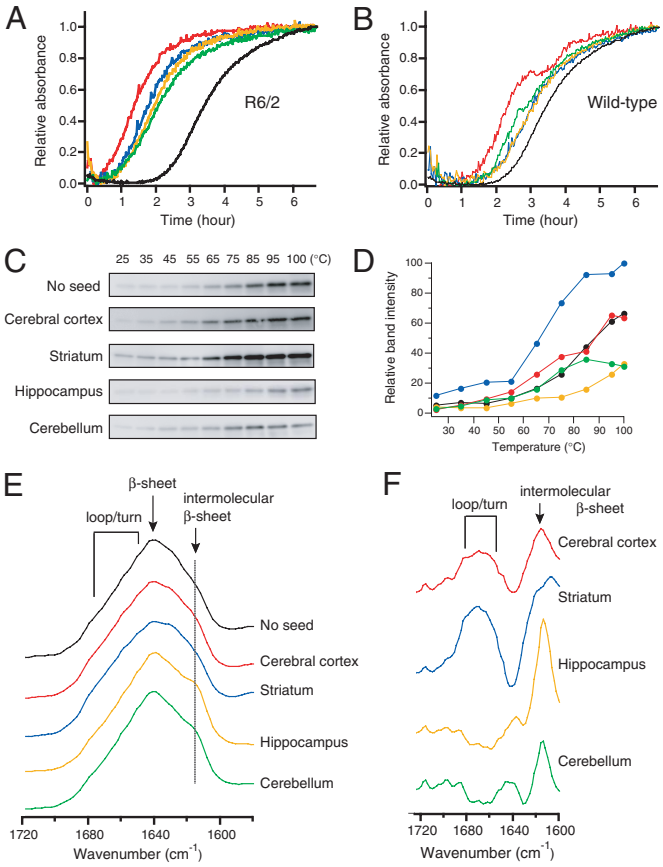

Fig. 3. thtt amyloids in different brain regions from R6/2 mice show distinct conformations. (*A* and *B*) Aggregation profile is shown of in vitro thttQ42 in the presence of thtt amyloids from R6/2 mice (*A*) or corresponding insoluble fractions from wild-type mice (*B*). Black, red, blue, yellow, and green lines show in vitro thttQ42 fibrillization in the absence (black) or presence of in vivo aggregates from cerebral cortex, striatum, hippocampus, and cerebellum, respectively. (*C*) Thermal stability of in vitro thttQ42 amyloids formed in the absence or presence of thtt amyloids from different brain regions of R6/2 mice. (*D*) The band intensity of thtt amyloids in different brain regions of R6/2 mice in *C* was plotted against temperature. (*E* and *F*) Structural analysis of thtt amyloids in different brain regions of R6/2 mice. (*E*) FT-IR spectra of in vitro thttQ42 amyloids formed in the absence or presence of thtt amyloids from different brain regions of R6/2 mice. (*F*) Difference FT-IR spectra obtained by subtraction of a spectrum of spontaneously formed thttQ42 (without seeds) from those of thttQ42 amyloids in different brain regions of R6/2 mice.

significantly accelerated the aggregation of thttQ150-GFP in neuro2a cells (Fig. 4*A*). Although thtt amyloids from all brain regions similarly enhanced thttQ150-GFP aggregation, the corresponding insoluble fraction from wild-type mouse brains exhibited only slight seeding effects. These results are consistent with the seeding experiments in vitro (Fig. 3 *A* and *B*) and verified that the thtt amyloids purified from R6/2 mice seed endogenous thttQ150-GFP in mammalian cells.

We then investigated whether the different conformations of thtt amyloids from R6/2 mice have distinct cytotoxic effects in thttQ150-GFP neuro2a cells. We found that the thtt amyloids from the striatum showed higher toxicity, whereas those from the hippocampus and cerebellum exhibited relatively mild toxic effects (Fig. 4*B*). The insoluble fraction from wild-type mouse brains showed no substantial toxic effects on the thttQ150-GFP neuro2a cells. Notably, the higher toxic effects of thermolabile thtt amyloids in striatum parallel those of the in vitro fragile thttQ42-4 °C amyloid conformation (Fig. 2*F*).

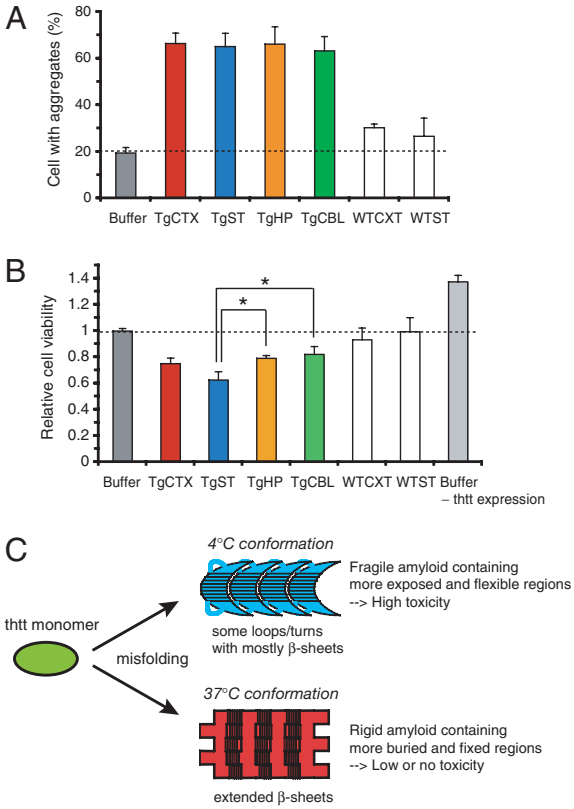

Fig. 4. Distinct conformations of thtt amyloids in different brain regions of R6/2 mice show distinct cytotoxicity in neuro2a cells. (*A* and *B*) Buffer alone or in vitro thttQ42 amyloids formed in the presence of thtt amyloids from different brain regions of R6/2 or WT mice were introduced into stable thttQ150-GFP neuro2a cells. The number of cells with thttQ150-GFP foci was counted after 15 h of thttQ150-GFP expression and cell differentiation (*A*), and cell viability was examined after 4 days by MTT assay (*B*). Tg, WT, CTX, ST, HP, and CBL denote R6/2 mice, wild-type mice, cerebral cortex, striatum, hippocampus, and cerebellum, respectively.*, $P < 0.05$. Values are mean ± SD. (*C*) A proposed mechanism of conformation-dependent cytotoxicity of thtt amyloid.

Discussion

The deposition of insoluble aggregates such as amyloids of causative proteins is a hallmark of many neurodegenerative disorders. Although it has recently been suggested that oligomeric species of aggregate-prone proteins are responsible for these diseases, it remains controversial as to whether amyloid itself is also toxic, simply a secondary manifestation of the pathology or rather a result of cellular protection (6, 7, 10–16). This apparent inconsistency of previous results regarding amyloid toxicity may result from the structural diversity of amyloid, as amyloid-forming protein often misfolds into multiple conformations and each conformation could exert distinct physiological effects (19, 23).

Previous reports indicate that the thermodynamic parameter of temperature can modulate protein folding and dynamics of amyloid-forming proteins, leading to different amyloid conformations (19, 32–34). Here we took advantages of this fact by making distinct thtt amyloids simply by polymerizing thtt protein at 4 °C or 37 °C. Furthermore, we developed a highly efficient procedure to introduce amyloid into mammalian cells. Although delivery of in vitro polyglutamines into mammalian cells has been reported (11, 14, 35), our efficient procedure of amyloid introduction in combination with creating distinct conformations of thtt amyloids allows us to directly evaluate toxicity of distinct amyloid conformations of thtt protein.

Both thtt-4 °C and thtt-37 °C aggregates showed the morphology of mature amyloids, which are different from protofibrils (Fig. 1*A*). The 2 amyloid conformations showed homogeneous and similar morphology by EM analysis and are abundant in β-sheets (4, 5, 36, 37) (Figs. 1 *B* and *C* and S2), which are intramolecular and/or intermolecular. However, we found some structural differences in the 2 amyloid conformations despite relatively low resolutional analyses. Notably, the 4 °C amyloid has some flexible loops/turns together with mostly β-sheets, including exposed polyglutamines, although it remains unclear whether the loop/turn structures are derived from expanded polyglutamiens or the rest of thtt. The 4 °C amyloid showed more toxic effects, whereas the 37 °C amyloid with extended β-sheets including buried polyglutamines showed less toxicity (Fig. 4*C*). It is possible that flexible and exposed polyglutamines easily interact with and sequester other functional proteins into thtt aggregates and thereby lead to cell death, whereas the limited dynamics of the polyglutamines buried into an amyloid core exerts only modest toxic or nontoxic effects. Thus, this study demonstrates that thtt amyloid can be either toxic or nontoxic, depending on their conformations. This finding is consistent with the previous observation that deposition of polyglutamine aggregates is not correlated with toxicity (16), as mature polyglutamine aggregates seen as deposition would be abundant in extended β-sheets and thus contain buried polyglutamines. Our results are also reconciled with the involvement of oligomeric and monomeric htt in cytotoxicity, as we and others have suggested important roles of exposed polyglutamines in oligomeric and monomeric htt in cytotoxicity (14, 28). Thus, the flexible and exposed property of expanded polyglutamines may be a critical determinant of cytotoxicity, regardless of whether the polyglutamine-bearing protein is in a monomeric, oligomeric, or amyloid form.

Another important issue in the field of neurodegenerative disorders is the regional specificity of cellular vulnerability (3). In HD, the striatum is the most vulnerable whereas loss of cerebellar Purkinje cells is limited only in juvenile-onset cases (2, 3). Nonetheless, it remains unclear what determines the regional specificity of HD. We hypothesized that structural differences of htt amyloids in distinct brain regions may be involved in the regional specificity of cellular vulnerability in HD. Here we showed that conformations of thtt amyloids in vivo were indeed diverse and led to different cytotoxicity. The higher toxicity of thtt amyloids in the striatum was also observed for the thtt-4 °C amyloid conformation in vitro. Importantly, both amyloid forms show similar structural features: They have β-sheets (but less extended β-sheets) with some loop/turn structures, resulting in relatively fragile and thermolabile conformations. In contrast, the rigid thtt amyloids, because of extended β-sheets, formed at 37 °C in vitro and in the hippocampus and cerebellum showed only mild toxicity. Consistent with these present results, striatal neurons are the most susceptible to neuronal death in HD (2). Therefore, the fragile and exposed property of thtt amyloid in striatum may be one of the key factors for striatal vulnerability in HD. These results suggest that the conformational differences of thtt amyloids (or soluble aggregated species) may dictate the regional specificity of HD. It is likely that different expression levels and types of chaperones and htt-interacting proteins in distinct brain regions modulate the extent of folding and dynamics of htt (38). These differences, in turn, could lead to a range of htt conformations that have distinct cytotoxicity when htt protein misfolds. In fact, microarray experiments show that mRNA levels of chaperones and transcription factors that bind to htt with expanded polyglutamines are different between distinct brain regions (39).

In summary, we demonstrated that thtt with expanded polyglutamines can misfold into multiple conformations and the structural diversity is involved in apparently different toxic effects of the amyloids. Although a range of efforts have been made to intervene with amyloid diseases (40), our finding provides a therapeutic strategy for polyglutamine disease: The conformation of 4 °C

amyloids should be targeted to prevent HD in the future. Furthermore, we propose that among different possible misfolding pathways of mutant htt, an attempt to direct the mutant htt to misfolding into a rigid amyloid conformation containing extended β-sheets could reduce the potential toxicity of the mutant htt.

Materials and Methods

Characterization of in Vitro thtt Amyloids. Preparation of thtt protein is described in the *SI Text*. Far-UV CD spectra of thtt amyloid (10 μM) in 5 mM potassium phosphate buffer containing 150 mM NaCl (pH 7.4) were measured by using a JASCO J-720 spectrophotometer at 25 °C. The spectra were an average of 4 scans recorded at a speed of 10 nm/min and a resolution of 0.1 nm. FT-IR spectra of thttQ42/62 amyloids were measured with 2 $BaCl_2$ windows in a Nicolet 6700 FT-IR spectrophotometer with a Nicolet Continuum microscope (Thermo Scientific) at room temperature under nitrogen gas. Spectral smoothing was applied with IgorPro (WaveMetrics) to increase the resolution. For structural analysis of thtt aggregates from R6/2 mice, 5 μM thttQ42 protein was polymerized at 4 °C in the presence of purified thtt aggregates (0.5 μg) and prescission protease, and the resulting amyloids were used for thermal stability and FT-IR analyses. Detailed procedures of the other biophysical methods are described in the *SI Text*.

Introduction of in Vitro thtt Amyloid into Neuro2a Cells. thttQ42/62 (5 μM) was polymerized at 4 °C or 37 °C, and resulting amyloid was collected by centrifugation at 20,000 $\times$ *g* for 30 min. After removal of supernatant, a 50 μM amyloid solution in 5 mM potassium phosphate buffer (pH7.4) containing 150 mM NaCl was sonicated for 30 s (Branson sonifier, 20%). Atomic force microscopy (Digital Instruments) showed that the sonicated fibers are homogeneous in length. An aliquot of the amyloid solution was mixed with Lipofectamine LTX and Plus reagents (Invitrogen) to the final concentration of 2.5 μM in 50 μL DMEM, according to the manufacturer's protocol. The mixture was incubated for 30 min at ambient temperature and poured onto stable neuro2a cells of an HD model (30) in 250 μL DMEM culture media. After 3 h of the amyloid transduction, expression of thtt-GFP was induced with 1 μM ponasterone A (Invitrogen), and cells were differentiated with 5 mM dibutyrylcyclic AMP (Nacalai Tesque).

Aggregate Counting and Cell Viability Assays. After 15 h of thtt expression and cell differentiation, we manually counted the number of cells ($\approx$200) with GFP foci of thtt aggregates under a fluorescence microscope. At this time, we did not observe cell death. Cell viability was determined by MTT cell count kit (Nacalai Tesque) after 4 days of the thtt expression and cell differentiation. Fluorescent and DIC images were acquired by FV1000-D confocal microscopy (Olympus). Statistical analyses ($n \geq 3$) were performed by Statview5.0 (SAS).

Purification of thtt Amyloids from R6/2 Mice. All experimental protocols involving mice were approved by the RIKEN Institutional Animal Care and Use Committee. Heterozygous thtt transgenic mice of R6/2 (31) were obtained from the Jackson Laboratory and maintained as previously reported (41). R6/2 transgenic and age-matched wild-type mice were transcardially perfused with ice-cold PBS and the brain was removed, followed by separation of cerebral cortex, striatum, hippocampus, and cerebellum. For purification of in vivo thtt aggregates, 0.35 g of each tissue (typically from 3, 12, 6, and 1 mice for cerebral cortex, striatum, hippocampus, and cerebellum, respectively) was homogenized with radioimmunoprecipitation assay buffer [100 mM Tris, 150 mM NaCl, 0.5% Triton X-100, protease inhibitor mixture (Roche), and 1 mM PMSF] by a digital homogenizer at 1,000 rpm, sonicated for 30 s (Branson sonifier, 20%) and ultracentrifuged at 540,000 $\times$ *g* for 30 min. The pellet was washed with 2% SDS repeatedly. The detailed procedure is described in *SI Text*.

ACKNOWLEDGMENTS. We thank Kuniko Kurihara for help with purification of thtt protein, Yuriko Sakamaki for EM analysis, Yumiko Ohashi for help with FT-IR experiments, Yoshiaki Furukawa for advice on fluorescent labeling of thtt protein, Gen Matsumoto (RIKEN Brain Science Institute, Japan) for providing PC12 cells, and RIKEN BSI-Olympus Collaboration Center for confocal imaging experiments. This study was partly supported by grants-in-aid from the Ministry of Education, Culture, Sports, Science and Technology, Japan (M.T. and N.N.), JST PRESTO (M.T.), Tekeda Science Foundation (M.T.), and Astellas Foundation for Research on Metabolic Disorders (M.T.).

1. Orr HT, Zoghbi HY (2007) Trinucleotide repeat disorders. *Annu Rev Neurosci* 30:575–621.
2. Vonsattel JP, DiFiglia M (1998) Huntington disease. *J Neuropathol Exp Neurol* 57:369–384.
3. Thomas EA (2006) Striatal specificity of gene expression dysregulation in Huntington's disease. *J Neurosci Res* 84:1151–1164.
4. Perutz MF, Johnson T, Suzuki M, Finch JT (1994) Glutamine repeats as polar zippers: Their possible role in inherited neurodegenerative diseases. *Proc Natl Acad Sci USA* 91:5355–5358.
5. Scherzinger E, et al. (1997) Huntingtin-encoded polyglutamine expansions form amyloid-like protein aggregates in vitro and in vivo. *Cell* 90:549–558.
6. Davies SW, et al. (1997) Formation of neuronal intranuclear inclusions underlies the neurological dysfunction in mice transgenic for the HD mutation. *Cell* 90:537–548.
7. DiFiglia M, et al. (1997) Aggregation of huntingtin in neuronal intranuclear inclusions and dystrophic neurites in brain. *Science* 277:1990–1993.
8. Bates G (2003) Huntingtin aggregation and toxicity in Huntington's disease. *Lancet* 361:1642–1644.
9. Ross CA, Poirier MA (2005) Opinion: What is the role of protein aggregation in neurodegeneration? *Nat Rev Mol Cell Biol* 6:891–898.
10. Ordway JM, et al. (1997) Ectopically expressed CAG repeats cause intranuclear inclusions and a progressive late onset neurological phenotype in the mouse. *Cell* 91:753–763.
11. Yang W, Dunlap JR, Andrews RB, Wetzel R (2002) Aggregated polyglutamine peptides delivered to nuclei are toxic to mammalian cells. *Hum Mol Genet* 11:2905–2917.
12. Saudou F, Finkbeiner S, Devys D, Greenberg ME (1998) Huntingtin acts in the nucleus to induce apoptosis but death does not correlate with the formation of intranuclear inclusions. *Cell* 95:55–66.
13. Klement IA, et al. (1998) Ataxin-1 nuclear localization and aggregation: Role in polyglutamine-induced disease in SCA1 transgenic mice. *Cell* 95:41–53.
14. Nagai Y, et al. (2007) A toxic monomeric conformer of the polyglutamine protein. *Nat Struct Mol Biol* 14:332–340.
15. Chimon S, et al. (2007) Evidence of fibril-like β-sheet structures in a neurotoxic amyloid intermediate of Alzheimer's β-amyloid. *Nat Struct Mol Biol* 14:1157–1164.
16. Arrasate M, Mitra S, Schweitzer ES, Segal MR, Finkbeiner S (2004) Inclusion body formation reduces levels of mutant huntingtin and the risk of neuronal death. *Nature* 431:805–810.
17. Haass C, Selkoe DJ (2007) Soluble protein oligomers in neurodegeneration: Lessons from the Alzheimer's amyloid β-peptide. *Nat Rev Mol Cell Biol* 8:101–112.
18. Dobson CM (2003) Protein folding and misfolding. *Nature* 426:884–890.
19. Chien P, Weissman JS, DePace AH (2004) Emerging principles of conformation-based prion inheritance. *Annu Rev Biochem* 73:617–656.
20. Eisenberg D, et al. (2006) The structural biology of protein aggregation diseases: Fundamental questions and some answers. *Acc Chem Res* 39:568–575.
21. Kodali R, Wetzel R (2007) Polymorphism in the intermediates and products of amyloid assembly. *Curr Opin Struct Biol* 17:48–57.
22. Shorter J, Lindquist S (2005) Prions as adaptive conduits of memory and inheritance. *Nat Rev Genet* 6:435–450.
23. Petkov AT, et al. (2005) Self-propagating, molecular-level polymorphism in Alzheimer's β-amyloid fibrils. *Science* 307:262–265.
24. Serpell LC, Berriman J, Jakes R, Goedert M, Crowther RA (2000) Fiber diffraction of synthetic α-synuclein filaments shows amyloid-like cross-β conformation. *Proc Natl Acad Sci USA* 97:4897–4902.
25. Ismail AA, Mantsch HH (1992) Salt bridge induced changes in the secondary structure of ionic polypeptides. *Biopolymers* 32:1181–1186.
26. Seshadri S, Khurana R, Fink AL (1999) Fourier transform infrared spectroscopy in analysis of protein deposits. *Methods Enzymol* 309:559–576.
27. Trottier Y, et al. (1995) Polyglutamine expansion as a pathological epitope in Huntington's disease and four dominant cerebellar ataxias. *Nature* 378:403–436.
28. Tanaka M, Machida Y, Nishikawa Y, Fujisawa T, Nukina N (2003) Formation of quasi-aggregates during fibrilization of polyglutamine proteins. *J Biol Chem* 278:34717–34724.
29. Peters-Libeu C, et al. (2005) Crystallization and diffraction properties of the Fab fragment of 3B5H10, an antibody specific for disease-causing polyglutamine stretches. *Acta Crystallogr F* 61:1065–1068.
30. Wang GH, et al. (1999) Caspase activation during apoptotic cell death induced by expanded polyglutamine in N2a cells. *Neuroreport* 10:2435–2438.
31. Mangiarini L, et al. (1996) Exon 1 of the HD gene with an expanded CAG repeat is sufficient to cause a progressive neurological phenotype in transgenic mice. *Cell* 87:493–506.
32. Mukhopadhyay S, Krishnan R, Lemke EA, Lindquist S, Deniz AA (2007) A natively unfolded yeast prion monomer adopts an ensemble of collapsed and rapidly fluctuating structures. *Proc Natl Acad Sci USA* 104:2649–2654.
33. Krishnan R, Lindquist SL (2005) Structural insights into a yeast prion illuminate nucleation and strain diversity. *Nature* 435:765–772.
34. Toyama BH, Kelly MJ, Gross JD, Weissman JS (2007) The structural basis of yeast prion strain variants. *Nature* 449:233–237.
35. Ren PH, et al. (2009) Cytoplasmic penetration and persistent infection of mammalian cells by polyglutamine aggregates. *Nat Cell Biol* 11:219–225.
36. Chen S, Berthelier V, Hamilton JB, O'Nuallain B, Wetzel R (2002) Amyloid-like features of polyglutamine aggregates and their assembly kinetics. *Biochemistry* 41:7391–7399.
37. Poirier MA, et al. (2002) Huntingtin spheroids and protofibrils as precursors in polyglutamine fibrilization. *J Biol Chem* 277:41032–41037.
38. Giadalevitz T, Ben-Zvi A, Ho KH, Brignull HR, Morimoto RI (2006) Progressive disruption of cellular protein folding in models of polyglutamine diseases. *Science* 311:1471–1474.
39. Hodges A, et al. (2006) Regional and cellular gene expression changes in human Huntington's disease brain. *Hum Mol Genet* 15:965–977.
40. Balch WE, Morimoto RI, Dillin A, Kelly JW (2008) Adapting proteostasis for disease intervention. *Science* 319:916–919.
41. Tanaka M, et al. (2004) Trehalose alleviates polyglutamine-mediated pathology in a mouse model of Huntington disease. *Nature Med* 10:148–154.